Functional Consequences of Preorganized Helical Structure in the Intrinsically Disordered Cell-Cycle Inhibitor p27^{Kip1}†

Ewa A. Bienkiewicz,[§,‡] Joshua N. Adkins,[§,‡] and Kevin J. Lumb*[,‡,⊥]

Department of Biochemistry and Molecular Biology, Department of Chemistry, Colorado State University, Fort Collins, Colorado 80523-1870, USA

Received September 11, 2001; Revised Manuscript Received November 5, 2001

ABSTRACT: p27^{Kip1} contributes to cell-cycle regulation by inhibiting cyclin-dependent kinase (Cdk) activity. The p27 Cdk-inhibition domain has an ordered conformation comprising an α-helix, a 3_{10} helix, and *β*-structure when bound to cyclin A-Cdk2. In contrast, the unbound p27 Cdk-inhibition domain is intrinsically disordered (natively unfolded) as shown by circular dichroism spectroscopy, lack of chemical-shift dispersion, and negative heteronuclear nuclear Overhauser effects. The intrinsic disorder is not due to the excision of the Cdk-inhibition domain from p27, since circular dichroism spectra of the full-length protein are also indicative of a largely unfolded protein. Both the inhibition domain and full-length p27 are active as cyclin A-Cdk2 inhibitors. Using circular dichroism and proline mutagenesis, we demonstrate that the unbound p27 Cdk-inhibition domain is not completely unfolded. The domain contains marginally stable helical structure that presages the α-helix, but not the 3_{10} helix, adopted upon binding cyclin A-Cdk2. Increasing or reducing the stability of the partially preformed α-helix in the isolated p27 domain with alanine or proline substitutions did not affect formation of the p27-inhibited cyclin A-Cdk2 complex in energetic terms. However, stabilization of the helix with alanine hindered kinetically the formation of the inhibited complex, suggesting that p27 derives a kinetic advantage from intrinsic structural disorder.

Many functional proteins involved in cellular processes such as the cell cycle, gene expression, and translation exhibit biophysical properties expected of unfolded, rather than folded, proteins (*1*, *2*). Such proteins have been variously called natively unfolded, intrinsically unstructured, or intrinsically disordered (*1*−*4*). Several intrinsically disordered proteins undergo protein folding disorder−order transitions upon binding target proteins or nucleic acids (*1*), indicating a functional requirement for organized structure for at least certain intrinsically disordered proteins. Molecular recognition by intrinsically disordered proteins is therefore analogous to protein folding in that a very large number of possible conformations converge to a well-defined structure.

p27^{Kip1} is a member of the p21 family of Cdk[1] inhibitors that negatively regulates the cell cycle and contributes to cellular growth and development (*5*−*7*). Human p27 contains an N-terminal Cdk-inhibition domain and a C-terminal domain of unknown function called the QT domain (*5*, *8*). The crystal structure of the human p27 Cdk-inhibition domain (residues 22−106) bound to human cyclin A-Cdk2 shows that residues 25−93 of p27 bind in an ordered conformation comprising two helices and elements of *β*-structure (Figure 1) (*9*). However, the p27 Cdk-inhibition

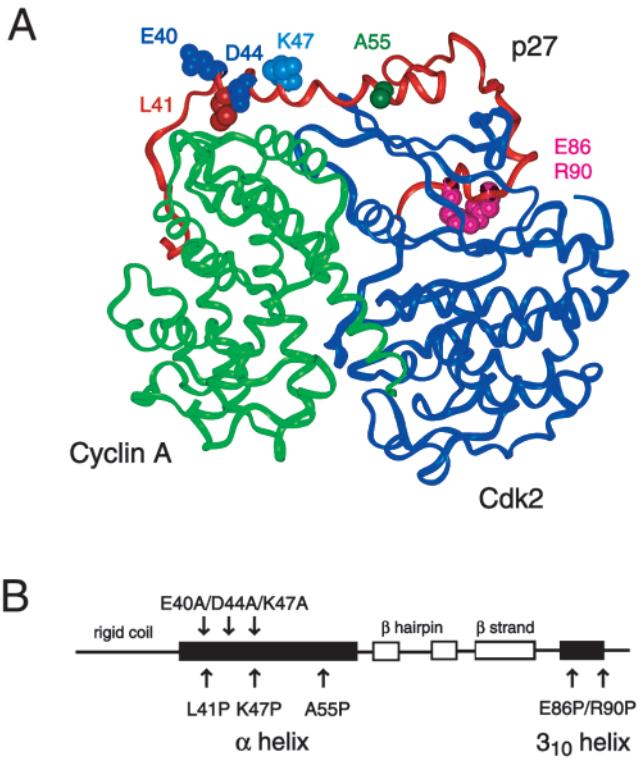

FIGURE 1: (A) The p27 Cdk-inhibition domain has a well-ordered conformation in the crystal structure of the p27-inhibited cyclin A-Cdk2 complex (*9*). Residues chosen for mutagenesis are shown using space-filling representations of the wild-type side chains. (B) Schematic representation of the secondary structure of the p27 Cdk-inhibition domain when bound to cyclin A-Cdk2. The α-helix is irregular between residues 51 and 53 (*9*).

† Supported by NIH (GM55156 and RR11981).

* Corresponding author: telephone: (970) 491-5440; fax: (970) 491-0494; e-mail lumb@lamar.colostate.edu.

‡ Department of Biochemistry and Molecular Biology.

⊥ Department of Chemistry.

§ E.A.B. performed mutagenesis and purification of p27ID proteins and carried out biophysical analysis. J.N.A. prepared the p27 Cdk2-binding domain, cyclin A, and Cdk2 and performed the functional analysis.

10.1021/bi015763t CCC: $22.00
Published on Web 12/19/2001

domain lacks an intramolecular hydrophobic core in the context of the cyclin A-Cdk2 complex (*9*), and circular dichroism and fluorescence spectra show that the unbound domain is largely unfolded in both ideal and thermodynamically nonideal, crowded solutions (*10*).

We report here a study of the functional consequences of conformational preferences in the intrinsically disordered human p27 Cdk-inhibition domain. Rather than existing as a random coil, the p27 Cdk-inhibition domain exhibits a propensity to form preexisting helical structure that corresponds to the α-helix, but not the 3_{10} helix, that forms upon binding cyclin A-Cdk2. Disruption of the preorganized α-helix in the unbound state by mutagenesis does not result in a significant thermodynamic or kinetic disadvantage to kinase inhibition. However, stabilization of the preformed helix by alanine mutagenesis decreases significantly the rate at which p27 inhibits cyclin A-Cdk2. These findings emphasize the importance of quaternary interactions during coupled folding and binding events and suggest that a biological advantage to intrinsic disorder is speed of molecular recognition.

METHODS

Protein Expression, Purification, and Mutagenesis. p27ID (corresponding to residues 22−97 of human p27 with an additional N-terminal Gly−Ser−His−Met) was expressed as a His-tag fusion protein. The expression vector for p27ID (called pET15b-p27ID) was constructed by ligating a PCR product encoding residues 22−97 of human p27 amplified from pET21a-p27 (*5*) into pET15b. The coding sequence was confirmed with dRhodamine automated sequencing. p27ID was expressed in *Escherichia coli* strain BL21 (DE3) grown in LB medium and purified from the soluble fraction of the cell lysate using His-bind resin (Novagen), and the His-tag was cleaved with thrombin (Novagen) (*11*, *12*). Final purification was by C_{18} HPLC using linear water/acetonitrile gradients containing 0.1% TFA. The identity of each p27ID preparation was confirmed with MALDI mass spectrometry, with the observed and expected masses agreeing to within 1 Da. Uniformly ^{15}N-labeled p27ID was prepared in the same way except that cells were grown in M9T minimal medium containing 1 g/L $(^{15}NH_4)_2SO_4$ (*13*).

Expression plasmids for p27ID mutants were prepared using the QuikChange PCR protocol (Stratagene), and the coding sequence for each plasmid was confirmed with dRhodamine automated sequencing. Mutants were expressed and purified in the same way as p27ID. The identity of each mutant protein was confirmed with MALDI mass spectrometry, with the observed and expected masses agreeing to within 2 Da.

$p27_{63-97}$ (corresponding to residues 63−97 of human p27) was prepared by endoproteinase AspN (Sigma P3303) digestion for 16 h at 25 °C of p27ID in 25 mM ammonium carbonate, 5% (v/v) acetonitrile, pH 7.8. Digest products were separated with C_4 HPLC using a linear water/acetonitrile gradient containing 0.1% TFA, and the desired peptide was identified with MALDI mass spectrometry (expected mass of 4246 Da; observed 4248 Da).

Human Cdk2 was expressed in baculovirus-infected High Five cells (*14*), and human cyclin A and p27 were expressed in *E. coli* strain BL21 (DE3) (*5*, *15*) as described elsewhere (*5*, *16*).

Concentration Determinations. Concentrations of stock solutions of p27ID (and mutants), $p27_{63-97}$, cyclin A, and Cdk2 were determined by absorbance in 6 M GuHCl using extinction coefficients at 280 nm of 15 220, 9530, 38 830, and 36 560 M^{-1} cm^{-1}, respectively (*17*). The concentration of full-length p27 was estimated from the absorbance at 280 nm in 25 mM HEPES, 150 mM NaCl, 5 mM $MgCl_2$, 0.05% NP-40, and 1 mM DTT, pH 7.7, using an extinction coefficient of 15 220 M^{-1} cm^{-1}.

Phosphorylation Assays. Cyclin A-Cdk2 activity was assayed by quantifying histone H1 phosphorylation (*15*) as described previously (*18*). Assays were performed in a total volume of 20 μL at 15 or 30 °C and at pH 7.5 in 25 mM HEPES, 50 mM NaCl, and 5 mM $MgCl_2$. Ten micrograms of calf thymus histone H1 (Gibco BRL 13221-015), 50 nM cyclin A-Cdk2, and the quantities of p27, p27ID, or p27ID mutants indicated in the figures were mixed and preincubated to allow formation of the inhibited complex before addition of 2.5 μCi [γ-^{33}P] ATP to initiate phosphorylation. Preincubation times of 5 to 60 min were used in experiments to determine the time to attain equilibrium (Figure 8). Preincubation times of 20 min (p27ID and the proline mutants) or 60 min (for the triple Ala mutant) were used in experiments to determine K_d values (Figure 9). Reactions were run for 20 min after initiation by the addition of ATP. The reaction was quenched with 5 μL of 50 mM Tris HCl, pH 6.8, 0.1% bromophenol blue, 2% SDS, and 10% glycerol and heating to 90 °C for 1 min. The solution was analyzed with denaturing (SDS) polyacrylamide gel electrophoresis, and the extent of histone H1 phosphorylation was quantified by autoradiography with a Molecular Dynamics PhosphorImager. The extent of inhibition was used as a measure of the extent of binding in a nonlinear least-squares fit to calculate K_d values for a 1:1 binding stoichiometry.

CD Spectroscopy. CD spectra of p27ID and p27ID mutants were collected with Jasco J720 and Aviv 202 spectrometers. Data were collected at least twice with reproducible results. Samples were prepared in kinase-assay buffer (25 mM HEPES, 50 mM NaCl, and 5 mM $MgCl_2$, pH 7.5) containing 1 mM DTT. Wavelength spectra were the average of 20 scans collected on samples in 0.1-mm path length cells containing 100 μM protein after equilibration at the data-collection temperature for 15 min. Thermal stability was monitored at protein concentrations of 50 μM from the change in $[\theta]_{222}$ as a function of temperature in a 2-mm path length cell. Samples were equilibrated at 0 °C for 15 min, and the temperature was then increased from 0 to 60 °C in steps of 2 °C with an equilibration time of 240 s and a data collection time of 90 s and decreased from 60 to 0 °C in steps of 4 °C with an equilibration time of 360 s and a data collection time of 90 s.

[1] Abbreviations: $[\theta]$, molar ellipticity; $[\theta]_{222}$, molar ellipticity at 222 nm; ATP, adenosine triphosphate; Cdk, cyclin-dependent kinase; Cdk2, cyclin-dependent kinase 2; CD, circular dichroism; DSS, 2,2-dimethyl-2-silapentane-5-sulfonate, sodium salt; DQF COSY, double quantum filtered correlation spectroscopy; DTT, dithiothreitol; GuHCl, guanidine hydrochloride; HPLC, high-performance liquid chromatography; K_d, dissociation constant; HSQC, heteronuclear single quantum correlation spectroscopy; LB, Luria-Bertani; MALDI, matrix-assisted laser desorption ionization; NOE, nuclear Overhauser effect; NMR, nuclear magnetic resonance; p27ID, biosynthetic protein corresponding to the Cdk-inhibition domain of human p27 (residues 22−97); PCR, polymerase chain reaction; SDS, sodium dodecyl sulfate; TFA, trifluoroacetic acid; TFE, trifluoroethanol; TOCSY, total correlation spectroscopy.

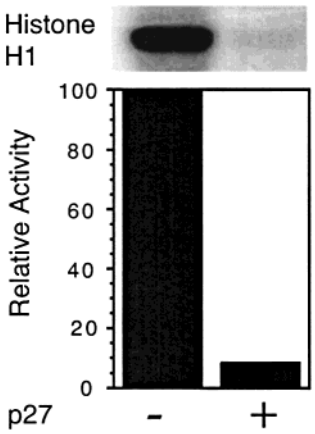

FIGURE 2: Full-length p27 inhibits histone H1 phosphorylation by cyclin A-Cdk2 (25 mM HEPES, 50 mM NaCl, and 5 mM $MgCl_2$, pH 7.5, 30 °C), in accord with previous results (*5*). Reactions contained 50 nM cyclin A-Cdk2 and 0 or ~50 nM p27. The cyclin A-Cdk2 used here is over 90% active, as calibrated with staurosporine (*16*).

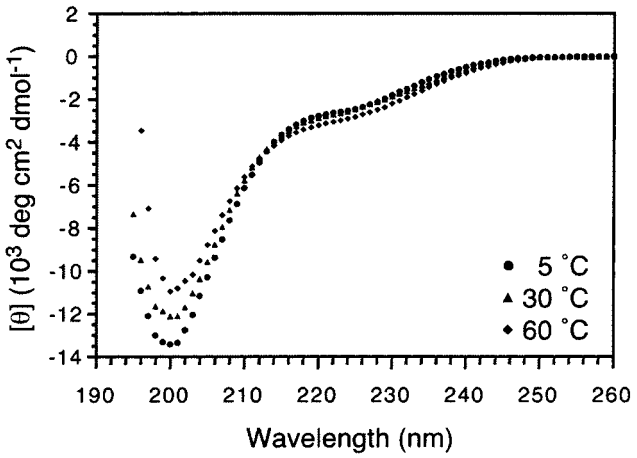

FIGURE 3: CD spectra of full-length p27 (25 mM HEPES, 150 mM NaCl, 5 mM $MgCl_2$, 0.05% NP-40, and 1 mM DTT, pH 7.7). The negative ellipticity at 200 nm and the lack of significant ellipticity at 216 nm and above are typical of the CD spectra of unfolded proteins.

CD wavelength spectra of full-length p27 were collected with a Jasco J720 spectrometer as described above. Samples contained 86 μM p27 in 25 mM HEPES, 150 mM NaCl, 5 mM $MgCl_2$, 0.05% NP-40, and 1 mM DTT, pH 7.7.

Helix content was estimated from $[\theta]_{222}$ by the method of Chen et al. (*19*) and with the program CDPro using basis set 7 and a wavelength range of 192−260 nm (*20*).

NMR Spectroscopy. NMR data were collected with a Varian Unity Inova operating at 500.1 MHz for ^{1}H. Samples contained 1 mM p27ID at pH 4.4 or 7.0 in kinase-assay buffer (25 mM HEPES, 50 mM NaCl, and 5 mM $MgCl_2$) containing 10 mM DTT. Experiments were performed at 30 °C. Spectra were referenced with internal DSS at zero ppm (*21*) and processed with NMRPipe (*22*). Gradient-enhanced DQF COSY (*23*), ^{1}H−^{15}N HSQC (*24*), and ^{15}N-edited TOCSY−HSQC (*25*) spectra consisted of 256 complex increments defined by 32 or 64 transients. Steady-state NOE values were measured with NMRView (*27*) from intensity changes in two-dimensional ^{1}H−^{15}N NOE correlation spectra (*26*). NOE correlation spectra consisted of 128 complex increments defined by 32 transients, collected with and without a 3 s ^{1}H saturation period using relaxation delays of 5 and 8 s, respectively.

RESULTS

Intrinsic Structural Disorder of p27. The full-length p27 used here inhibits histone H1 phosphorylation by cyclin A-Cdk2 (Figure 2). The CD spectrum of full-length human p27 is characteristic of an unfolded protein (Figure 3). The minimum at 200 nm is indicative of an unfolded conformation, and the weak negative shoulder at 222 nm suggests the absence of significant amounts of helix or β-strand. The helix content is estimated at 2 or 6% from $[\theta]_{222}$ or CDPro, respectively. The results indicate that full-length p27, while active as a Cdk inhibitor, is largely unfolded.

Intrinsic Structural Disorder of the p27 Cdk-Inhibition Domain. p27ID corresponds to residues 22 to 97 of human p27. This region of p27 has an ordered structure when bound to cyclin A-Cdk2 (Figure 1A). Cyclin A-Cdk2 is approximately 90% inhibited by equimolar p27ID at 30 °C (Figure 4), in accord with the 1:1 inhibition stoichiometry

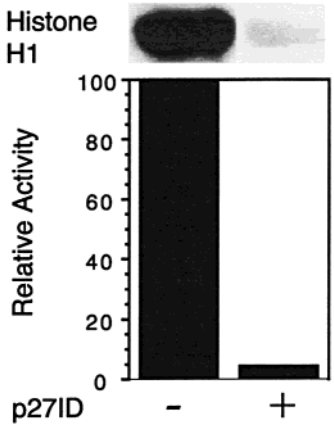

FIGURE 4: p27ID inhibits histone H1 phosphorylation by cyclin A-Cdk2 (25 mM HEPES, 50 mM NaCl, and 5 mM $MgCl_2$, pH 7.5, 30 °C). Reactions contained 50 nM cyclin A-Cdk2 and 0 or 50 nM p27ID. The cyclin A-Cdk2 used here is over 90% active, as calibrated with staurosporine (*16*).

observed in the crystal structure (Figure 1A). If p27ID were substantially inactive, then the apparent molar ratio of p27ID to cyclin A-Cdk2 for essentially complete inhibition would exceed 1:1, given that the cyclin A-Cdk2 used here is over 90% active, as calibrated with staurosporine.

The NMR properties of p27ID at 30 °C are characteristic of an unfolded protein. ^{1}H chemical-shift ranges were obtained from DQF COSY (pH 4.4) or TOCSY−HSQC (pH 7.0) spectra using gradients for solvent suppression. The H^{α} and H^{N} chemical shifts at pH 4.4 span 3.9−4.6 and 7.8−8.6 ppm, respectively, and at pH 7.0 span 4.05−4.59 and 7.77−8.58 ppm, respectively (data not shown). These chemical-shift ranges are typical of those observed in unfolded proteins (*28*). The amide ^{1}H−^{15}N NOE is negative (approximately −1 to −3.9) for each of 64 resolved mainchain amide cross-peaks at pH 4.4 (from an expected total of 70; data not shown), indicating that the p27ID main chain is highly flexible with motion on a time scale characteristic of unfolded proteins (*29*, *30*).

The CD spectra of p27ID in kinase-assay buffer at 30 and 60 °C are also characteristic of an unfolded protein (Figure 5). The minimum at 204 nm is indicative of an unfolded

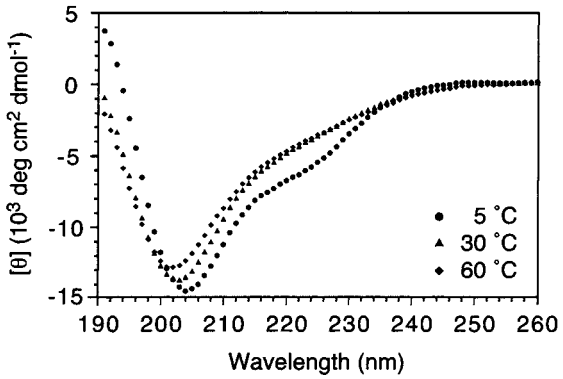

FIGURE 5: CD spectra of p27ID in kinase-assay buffer (25 mM HEPES, 50 mM NaCl, and 5 mM $MgCl_2$, pH 7.5) containing 1 mM DTT. At both 30 and 60 °C, the negative ellipticity at 200 nm and the lack of significant ellipticity at 216 nm and above are typical of the CD spectra of unfolded proteins. At 5 °C, the signal at 222 nm becomes more negative, consistent with an increase in helix stability at lower temperature.

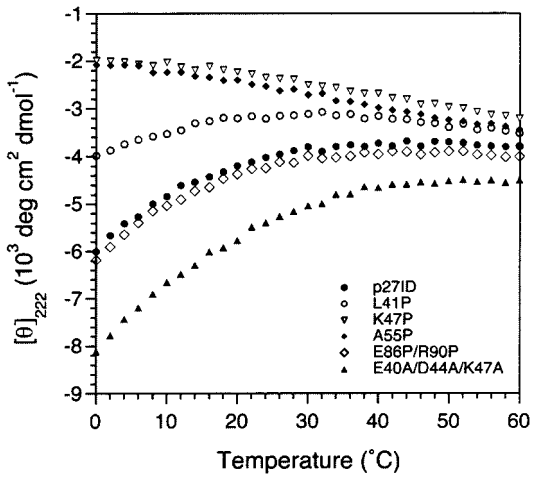

FIGURE 6: Temperature dependence of $[\theta]_{222}$ of p27ID and the mutants in kinase-assay buffer (25 mM HEPES, 50 mM NaCl, and 5 mM $MgCl_2$, pH 7.5) containing 1 mM DTT. Changes in $[\theta]_{222}$ were reversible (the folding and unfolding curves were essentially superimposable, with at least 90% of the starting signal regained on cooling, with the exception of the E86P/R90P mutant which regained approximately 85% of the starting signal on cooling).

conformation, and the weak negative shoulder at 222 nm suggests the absence of significant amounts of helix or β-strand. The CD spectrum of p27ID at 25 °C is independent of pH in the range 4 to 7.5 and concentration in the range 20 μM to 1 mM (data not shown). The spectroscopic data collectively indicate that the p27 Cdk-inhibition domain is intrinsically disordered in isolation under conditions where the domain is functional as a kinase inhibitor, in contrast to the ordered structure adopted upon binding cyclin A-Cdk2 (Figure 1A).

Local Helix Formation in the p27 Cdk-Inhibition Domain. CD spectroscopy indicates that p27ID becomes partially helical at lower temperature (Figure 5). The lack of a folded baseline and differing estimates of $[\theta]_{222}$ for a fully formed helix hinder quantitative determinations of helical content in largely unfolded proteins such as p27ID. Using the method of Chen et al. (*19*) and CDPro (*20*), the helix content of p27ID at 5 °C is estimated to be 10 and 16%, respectively. Both estimates are less than the total α and 3_{10} helix content of 33% observed in the crystal structure of the domain bound to cyclin A-Cdk2 (*9*). The temperature dependence of the CD signal at 222 nm indicates that the helix is only marginally stable (Figure 6). Thus, although intrinsically disordered at physiological temperature, p27ID exhibits an inherent propensity to adopt helical structure.

Helix Localization by Proline Mutagenesis. CD cannot determine directly if the helix observed at low temperature corresponds to the two regions of p27 that adopt stable helices upon binding cyclin A-Cdk2. Although single proline residues can be accommodated in helices of folded proteins with some local distortion (*31*), proline greatly destabilizes isolated helices (*32*). Proline mutations are therefore expected to disrupt helix formation in the unbound p27 Cdk-inhibition domain if placed in regions that adopt helical conformations, but to have little or no effect on helix content if placed in unfolded regions (*33*, *34*).

p27 forms two helical regions upon binding cyclin A-Cdk2: an α-helix comprising residues 38 to 59, and a 3_{10} helix comprising residues 85−90 (Figure 1A). Three residues of high intrinsic helical propensity (*32*) in the α-helix (Leu 41, Lys 47, and Ala 55) were substituted individually with Pro. The Lys 47 and Ala 55 side chains project away from cyclin A-Cdk2, whereas Leu 41 contacts cyclin A (Figure 1A). The three aromatic residues at the center of the 3_{10} helix were not changed, since mutation of aromatic residues can affect CD spectra regardless of any change in secondary structure (*35*). Instead, Glu 86 and Arg 90 were mutated together to proline to disrupt main chain hydrogen bonding within the 3_{10} helix. If either the α or the 3_{10} helices are partially populated at low temperature, then the proline mutations would be expected to destabilize the helix and decrease the helical component of the CD spectrum.

CD indicates that proline substitutions in the region of p27 that adopts α-helix upon binding cyclin A-Cdk2 diminish the helix content of unbound p27ID. Helix formation at 5 °C in the K47P and A55P mutants is essentially abolished, as judged by the decrease in the amplitude of the CD signal at 222 nm (Figure 7A). The CD signal at 222 nm becomes more negative with increasing temperature (Figure 6), which is the opposite behavior expected for thermally induced unfolding of helices and is typical of unfolded or extended conformations (*36*). The L41P mutation is less destabilizing (Figure 6) and reduces the helix content approximately 2-fold at 5 °C (Figure 7A), which is consistent with its position in the first turn of the helix. The proline substitutions in the region of p27 that adopts the 3_{10} helix upon binding cyclin A-Cdk2 have no significant effect on helix formation (Figures 6 and 7).

The proline substitutions map the marginally stable helix observed with CD at low temperature to the region of p27 that forms the α-helix upon binding cyclin A-Cdk2. At 30 °C, the CD signal at 222 nm (indicative of helix formation) is slightly less negative for the L41P, K47P, and A55P mutants, suggesting that the helix is present to some extent in the wild-type domain even at 30 °C (Figure 7B). In contrast, the 3_{10} helix is not populated in the isolated p27 Cdk-inhibition domain even at low temperature.

Contribution of Local Helix Formation to Cdk Inhibition. If the incipient α-helix of p27 contributes significantly to the specificity of the interaction between p27 and cyclin A-Cdk2, then the ability of the L41P, K47P, and A55P

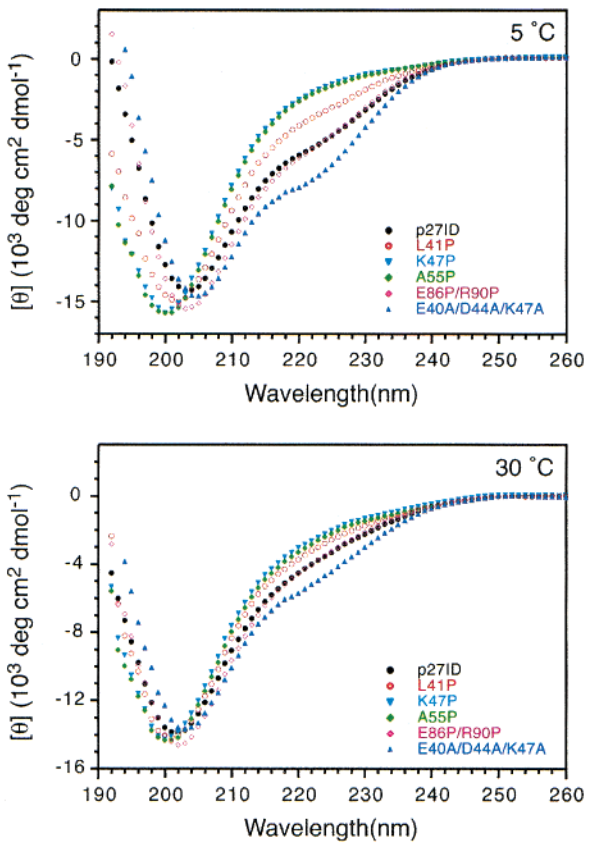

FIGURE 7: CD spectra of p27ID and the mutants in kinase-assay buffer (25 mM HEPES, 50 mM NaCl, and 5 mM $MgCl_2$, pH 7.5) containing 1 mM DTT at (top) 5 °C and (bottom) 30 °C. A negative or positive change in $[\theta]_{222}$ upon mutagenesis reflects an increase or decrease in helix content, respectively.

mutants to inhibit cyclin A-Cdk2 will be compromised. Dissociation constants (K_d) were determined with cyclin A-Cdk2 inhibition assays.

The time for p27ID and the proline mutants to attain equilibrium upon binding cyclin A-Cdk2 was monitored by following the decrease in activity of cyclin A-Cdk2 after preincubation with a 50% mol equivalent of p27ID and the L41P, K47P, A55P, and E86P/R90P mutants for 5 to 60 min (Figure 8). The formation of complexes of p27ID and the proline mutants with cyclin A-Cdk2 is at equilibrium under these conditions within 10 min (Figure 8).

p27ID binds cyclin A-Cdk2 with a K_d of 8 ± 2 nM at 30 °C (Figure 9). The L41P mutant, which contains approximately half of the helix in unbound p27ID, binds with essentially the same affinity (K_d = 9 ± 1 nM at 30 °C) as p27ID. The K47P and A55P mutants, in which helix formation is essentially abolished, bind with slightly lower affinities (16 ± 3 and 13 ± 2 nM, respectively, at 30 °C). At 15 °C, where the helix is more populated, the K_d values for p27ID and L41P are 8 ± 1 and 10 ± 2 nM, respectively (data not shown). Thus, some correlation exists between loss of α-helix in the unbound inhibitor and an increase in K_d. However, the differences are very small in free energy terms ($\Delta\Delta G$ = 0.1 to 0.4 ± 0.4 kcal mol^{-1}) as compared to the free energy of binding (ΔG = −11.4 ± 0.3 kcal mol^{-1} for p27ID).

The E86P/R90P double mutation does not reduce the helix content of unbound p27ID, but does increase the K_d at 30 °C to 14 ± 2 nM ($\Delta\Delta G$ = 0.3 ± 0.2 kcal mol^{-1} relative to

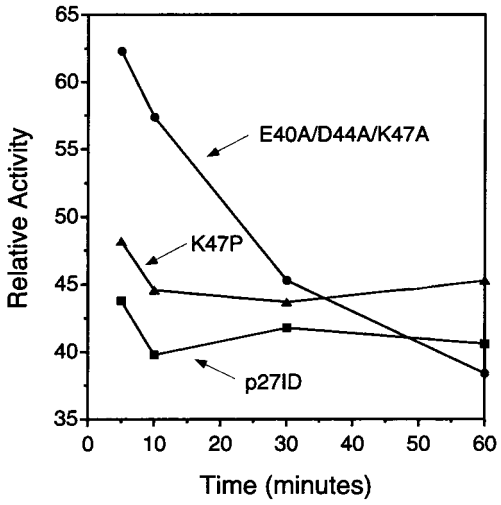

FIGURE 8: Time to attain equilibrium (50 nM cyclin A-Cdk2, 25 mM HEPES, 50 mM NaCl, and 5 mM $MgCl_2$, pH 7.5, 30 °C). Data are shown in terms of relative activity where the activity of cyclin A-Cdk2 in the absence of inhibitor is assigned an activity of 100. In the presence of a 50% mol equivalent of inhibitor, the relative activity would be 50, if the proteins were equally active. After 10 min, the activity of cyclin A-Cdk2 is reduced to 45 ± 5 by p27ID and the single mutants. In contrast, it takes at least 30 min for the E40A/D44A/K47A mutant to reduce the relative activity of cyclin A-Cdk2 to the anticipated value of 50. Accordingly, K_d determinations were made using a preincubation time of 20 min for p27ID and the L41P, K47P, A55P mutants and 60 min for the triple-Ala mutant. Experiments were repeated four times for p27ID and the K47P and E40A/D44A/K47A mutants and twice for the L41P, A55P, and E86P/R90P mutants (data not shown) with reproducible results. The error in each point is ± 10%.

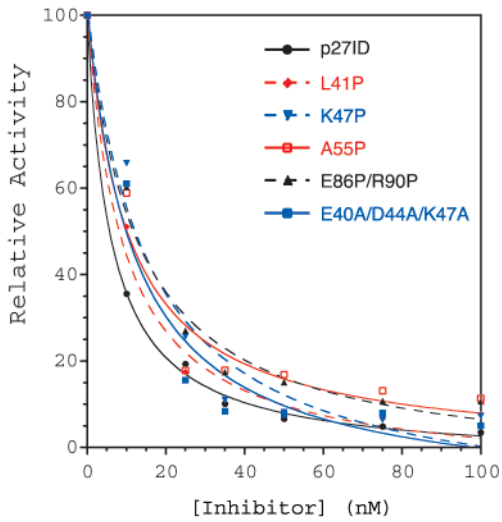

FIGURE 9: K_d determinations from cyclin A-Cdk2 inhibition assays (50 nM cyclin A-Cdk2, 25 mM HEPES, 50 mM NaCl, and 5 mM $MgCl_2$, pH 7.5, 30 °C). Experiments were performed six times with reproducible results.

p27ID; Figure 9). Since the helix content is unperturbed by the E86P/R90P mutations, the change in affinity likely reflects disruption of the quaternary contacts between the mutated residues of p27ID and Cdk2, including hydrogen bonds involving Arg 90 of p27 and Gln 131 and Asn 132 of Cdk2 (*9*).

A peptide corresponding to just the Cdk2-binding domain of p27 ($p27_{63-97}$) does not inhibit cyclin A-Cdk2 (data not shown), in accord with previous studies (*5*). This result rules out the possibility that just the Cdk2-binding regions of either

p27ID or the proline mutants are sufficient to inhibit cyclin A-Cdk2 under the conditions used here.

Helix Stabilization with Alanine Substitutions. The importance of preformed local helix formation can be addressed by stabilizing helices with multiple alanine substitutions (*37*).[2] Three sites in the α-helix (Gln 40, Asp 44, and Lys 47) were substituted simultaneously with Ala. These residues do not make quaternary contacts with cyclin A-Cdk2 in the crystal structure (*9*), and AGADIR (*38*, *39*) predicts a 50−100% increase in helix content for residues 38−52 of the α-helix upon their simultaneous substitution with Ala. CD spectroscopy indicates that helix content of the E40A/D44A/K47A mutant is increased as envisaged (Figures 6 and 7), with an estimated helix content at 5 °C of 17 or 22% from $[\theta]_{222}$ or CDPro, respectively. The expected value would be 29% if the α-helix (but not the 3_{10} helix) was fully formed in the mutant (Figure 1B) (*9*). The K_d of the E40A/D44A/K47A mutant for cyclin A-Cdk2 is increased slightly to 12 ± 3 nM ($\Delta\Delta G = 0.4 \pm 0.2$ kcal mol^{-1} relative to p27ID; Figure 9).

The results for the E40A/D44A/K47A mutant indicate that stabilization of the incipient α-helix in unbound p27 does not lead to a corresponding increase in the stability of the complex, and indeed leads to a slight destabilization of the complex in free energy terms. Studies of the time course of inhibition indicate that the E40A/D44A/K47A mutant complex takes approximately three times longer than the p27ID or the single-proline mutants to reach equilibrium (Figure 8). Thus, stabilization of helical structure with Ala mutagenesis in the otherwise disordered p27 results in a kinetic impediment to kinase inhibition.

DISCUSSION

The Cdk-inhibition domain of p27 has an ordered structure when bound to cyclin A-Cdk2 (Figure 1A). In the unbound state, however, the domain is intrinsically disordered. p27 binding is therefore coupled with folding. The intrinsic disorder is not due to excision of the inhibition domain from the full-length protein since full-length p27 is also largely unfolded.

The Cdk-inhibition domains of $p21^{Cip1/Waf1}$ and $p57^{Kip2}$ are also intrinsically disordered or unfolded (*18*, *40*). The human p27 Cdk-inhibition domain (residues 22−97) shares 36 and 33% sequence identity with the corresponding regions of human p21 and p57, respectively (*5*, *8*, *41*−*43*). Such sequence identity between folded proteins the size of the Cdk-inhibition domains would suggest strongly that the proteins have similar structures (*44*). Likewise, it is intuitively reasonable that sequence identity with a known disordered protein would be a reliable predictor of intrinsic disorder, and this is the case for at least the p21 family of Cdk-inhibition domains (*18*).

The primary sequences of both p27ID and full-length p27 are depleted in hydrophobic residues and enriched in Pro, Glu, Lys, and Arg, relative to the average amino acid composition of proteins in the SWISS−PROT database (*51*). The deviations in amino acid composition are consistent with the intrinsic disorder of p27ID and p27 (*18*, *52*, *53*).

The p27 inhibition domain is not completely unfolded or unstructured. Instead, the domain exhibits a propensity to form marginally stable helical structure that presages the α-helix adopted upon binding cyclin A-Cdk2. The p27 Cdk-inhibition domain, therefore, samples both local helical and unfolded structures as opposed to existing as a random-coil ensemble that lacks local conformational preferences. Analogous observations have been made of low levels of native-like residual structure in peptide fragments and denatured proteins (*45*) and in other intrinsically disordered proteins (*46*−*50*).

It is intuitively reasonable that preformed secondary structure in intrinsically disordered proteins will contribute favorably to stability during coupled folding and binding events. For example, mutations that increase helical propensity in regions that adopt helices in the native structure stabilize the folded state of a number of monomeric and dimeric proteins by approximately 1 to 9 kcal/mol (*37*, *54*−*56*). For p27, however, both disruption and stabilization by mutagenesis of the incipient α-helix in the unbound Cdk-inhibition domain leads to only a marginal decrease (<0.5 kcal mol^{-1}) in the stability of the inhibited cyclin A-Cdk2 complex. These losses in stability upon mutagenesis of residues within the α and 3_{10} helices are small when compared to the binding free energy of −11.4 kcal mol^{-1} for the wild-type complex. This observation indicates that nonlocal (quaternary) contacts between p27 and cyclin A-Cdk2 overwhelm any contribution of preformed local (α-helical) structure in unbound p27 to the free energy of p27 binding to cyclin A-Cdk2. Indeed, qualitative results from point or deletion mutagenesis studies of p27 and cyclin A suggest that a significant fraction of the binding free energy is embodied in quaternary interactions between cyclin A and p27 in the N-terminal rigid-coil region of the p27 inhibition domain (*5*, *57*).

Preorganized, native-like local (secondary) structure formation in unbound disordered proteins that presages the folded structure formed upon binding may contribute favorably to the rate of binding. An example is the coupled dimerization and folding of the GCN4 leucine zipper, where mutations that increase secondary structure propensities accelerate folding (*37*). For p27, however, disruption of the preformed α-helix by proline mutagenesis does not affect significantly the rate of complex formation as reflected by the time to form the bound complex. Indeed, stabilization of the α-helix in unbound p27 with three alanine substitutions (E40A/D44A/K47A) slows by approximately 3-fold the rate of formation of the inhibited complex. It has been previously noted that stabilization of nonnative helical structure in the unfolded state can slow protein folding (*58*, *59*). Such observations may be relevant here, since the α-helix of p27 is irregular between residues 51 and 53 when bound to cyclin A-Cdk2 (Figure 1A). Although our current data address changes in the overall rate, rather than individual association or dissociation rate constants, stabilization of a continuous α-helix in this region of unbound p27 could introduce a

[2] TFE has also been used to stabilize helices (*67*). TFE induces changes in the CD spectrum of p27ID that are indicative of helix formation (*10*). Analysis of CD spectra with the method of Chen et al. (*19*) suggests that 30 and 93% (v/v) TFE increases the helical content of p27ID to approximately 50 and 60%, respectively (E.A.B. and K.J.L., unpublished results). The helix content determined with CDPro (*20*) is approximately 5% higher. Both estimates of helix content from the CD data exceed that observed upon binding cyclin A-Cdk2 (*9*), suggesting that TFE stabilizes helical structure in p27 that is irrelevant to the conformation of p27 when bound to cyclin A-Cdk2.

requirement for disruption of the helix prior to binding, with a concomitant decrease in the rate of complex formation. Alternatively, mutation of the charged residues of the E40A/D44A/K47A mutant may disrupt a kinetic advantage due to electrostatic interactions (*60*). Regardless of the origin of the kinetic impediment to the E40A/D44A/K47A mutant, the results indicate that the lack of preformed α-helix contributes beneficially to the rate at which p27 inhibits kinase activity.

Different models for protein folding place different weights on the importance of local (secondary) structure, with framework or hierarchical models emphasizing early formation of secondary structure (*61*, *62*) and subdomain or nucleation mechanisms highlighting tertiary (and quaternary) interactions that stabilize marginally stable secondary structure elements (*63*−*66*). Both viewpoints are supported by experimental observations, which certainly reflects a context dependence of the relative importance of local and nonlocal interactions during folding. For p27, the linked process of folding and binding is more akin to a protein-folding mechanism in which the formation of nonlocal tertiary or quaternary interactions is more significant in energetic and kinetic terms than local (secondary structure) formation.

We conclude that the unbound p27 Cdk-inhibition domain is largely unfolded with a detectable conformational bias toward the α-helix formed upon binding cyclin A-Cdk2. This conformational bias is not beneficial in thermodynamic or kinetic terms for productive folding and binding. Indeed, enhancement of the propensity to form the α-helix impedes kinase inhibition in kinetic terms. It is tempting to speculate that intrinsic disorder in certain regulatory proteins imparts the evolutionary advantage of a rapid response to extracellular stimuli or cell damage.

ACKNOWLEDGMENT

We thank J. W. Harper and J. Massagué for plasmids, D. O. Morgan for the Cdk2 baculovirus, A. J. Kennan and R. W. Woody for use of CD spectrometers, and K. M. Campbell, H. A. Giebler, C. D. Rithner, and R. W. Woody for discussions.

REFERENCES

1. Wright, P. E., and Dyson, H. J. (1999) *J. Mol. Biol. 293*, 321−331.
2. Dunker, A. K., Lawson, J. D., Brown, C. J., Williams, R. M., Romero, P., Oh, J. S., Oldfield, C. J., Campen, A. M., Ratliff, C. M., Hipps, K. W., Ausio, J., Nissen, M. S., Reeves, R., Kang, C., Kissinger, C. R., Bailey, R. W., Griswold, M. D., Chiu, W., Garner, E. C., and Obradovic, Z. (2001) *J. Mol. Graph. Model. 19*, 26−59.
3. Weinreb, P. H., Zhen, W., Poon, A. W., Conway, K. A., and Lansbury, P. T. (1996) *Biochemistry 35*, 13709−13715.
4. Campbell, K. M., Terrell, A. R., Laybourn, P. J., and Lumb, K. J. (2000) *Biochemistry 39*, 2708−2713.
5. Polyak, K., Lee, M., Erdjument-Bromage, H., Koff, A., Roberts, J. M., Tempst, P., and Massagué, J. (1994) *Cell 78*, 59−66.
6. Toyoshima, H., and Hunter, T. (1994) *Cell 78*, 67−74.
7. Vidal, A., and Koff, A. (2000) *Gene 247*, 1−15.
8. Matsuoka, S., Edwards, M. C., Bai, C., Parker, S., Zhang, P., Baldini, A., Harper, J. W., and Elledge, S. J. (1995) *Genes Dev. 9*, 650−662.
9. Russo, A. A., Jeffrey, P. D., Patten, A. K., Massagué, J., and Pavletich, N. P. (1996) *Nature 382*, 325−331.
10. Flaugh, S. L., and Lumb, K. J. (2001) *Biomacromolecules 2*, 538−540.
11. Novagen Technical Bulletin TB188 (1998) *Thrombin Kits*.
12. Novagen Technical Bulletin TB054 (2001) *His-Bind Kits*.
13. McIntosh, L. P., Griffey, R. H., Muchmore, D. C., Nielson, C. P., Redfield, A. G., and Dahlquist, F. W. (1987) *Proc. Natl. Acad. Sci. U.S.A. 84*, 1244−1248.
14. Desai, D., Gu, Y., and Morgan, D. O. (1992) *Mol. Cell. Biol. 3*, 571−582.
15. Connell-Crowley, L., Solomon, M. J., Wei, N., and Harper, J. W. (1993) *Mol. Biol. Cell 4*, 79−92.
16. Adkins, J. N., and Lumb, K. J. (2000) *Biochemistry 39*, 13925−13930.
17. Edelhoch, H. (1967) *Biochemistry 6*, 1948−1954.
18. Adkins, J. N., and Lumb, K. J. (2002) *Proteins 46*, 1−7.
19. Chen, Y., Yang, J. T., and Martinez, H. M. (1972) *Biochemistry 11*, 4120−4131.
20. Sreerama, N., and Woody, R. W. (2000) *Anal. Biochem. 287*, 252−260.
21. Wishart, D. S., Bigam, C. G., Yao, J., Abildgaard, F., Dyson, H. J., Oldfield, E., Markley, J. L., and Sykes, B. D. (1995) *J. Biomol. NMR 6*, 135−140.
22. Delaglio, F., Grzesiek, S., Vuister, G. W., Zhu, G., Pfeifer, J., and Bax, A. (1995) *J. Biomol. NMR 6*, 277−293.
23. van Zijl, P. C. M., Johnson, M. O., Mori, S., and Hurd, R. E. (1995) *J. Magn. Reson. A113*, 265−270.
24. Kay, L. E., Keifer, P., and Saarinen, T. (1992) *J. Am. Chem. Soc. 114*, 10663−10665.
25. Zhang, O., Kay, L. E., Olivier, J. P., and Forman-Kay, J. D. (1994) *J. Biomol. NMR 4*, 845−858.
26. Farrow, N. A., Muhandiram, R., Singer, A. U., Pascal, S. M., Kay, C. M., Gisg, G., Shoelson, S. E., Pawson, T., Forman-Kay, J. D., and Kay, L. E. (1994) *Biochemistry 33*, 5984−6003.
27. Johnson, B. A., and Blevins, R. A. (1994) *J. Biomol. NMR 4*, 603−614.
28. Wishart, D., and Case, D. A. (2001) *Methods Enzymol. 338*, 3−34.
29. Cho, H. S., Liu, C. W., Damberger, F. F., Pelton, J. G., Nelson, H. C., and Wemmer, D. E. (1996) *Protein Sci. 5*, 262−269.
30. Muchmore, S. W., Sattler, M., Liang, H., Meadows, R. P., Harlan, J. E., Yoon, H. S., Nettesheim, D., Chang, B. S., Thompson, C. B., Wong, S., Ng, S., and Fesik, S. W. (1996) *Nature 381*, 335−341.
31. Barlow, D. J., and Thornton, J. M. (1988) *J. Mol. Biol. 201*, 601−619.
32. Serrano, L. (2000) *Adv. Protein Chem. 53*, 49−85.
33. Schulman, B. A., and Kim, P. S. (1996) *Nat. Struct. Biol. 3*, 682−687.
34. Gursky, O. (2001) *Biochemistry 40*, 12178−12185.
35. Woody, R. W., and Dunker, A. K. (1996) in *Circular Dichroism and the Conformational Analysis of Biomolecules* (Fasman, G. D., Ed.) pp 109−157, Plenum Press, New York.
36. Woody, R. W. (1992) *Adv. Biophys. Chem. 2*, 37−79.
37. Zitzewitz, J. A., Ibarra-Molero, B., Fishel, D. R., Terry, K. L., and Matthews, C. R. (2000) *J. Mol. Biol. 296*, 1105−1116.
38. http://www.embl-heidelberg.de/Services/serrano/agadir/agadir-start.html.
39. Lacroix, E., Viguera, A. R., and Serrano, L. (1998) *J. Mol. Biol. 284*, 173−191.
40. Kriwacki, R. W., Hengst, L., Tennant, L., Reed, S. I., and Wright, P. E. (1996) *Proc. Natl. Acad. Sci. U.S.A. 93*, 11504−11509.
41. Harper, J. W., Adami, G. R., Wei, N., Keyomarsi, K., and Elledge, S. J. (1993) *Cell 75*, 805−816.
42. Xiong, Y., Hannon, G. J., Zhang, H., Casso, D., Kobayashi, R., and Beach, D. (1993) *Nature 366*, 701−704.
43. El-Deiry, W. S., Tokino, T., Velculescu, V. E., Levy, D. B., Parsons, R., Trent, J. M., Lin, D., Mercer, W. E., Kinzler, K. W., and Vogelstein, B. (1993) *Cell 75*, 817−825.
44. Chothia, C., and Lesk, A. M. (1986) *EMBO J. 5*, 823−826.
45. Dyson, H. J., and Wright, P. E. (1996) *Annu. Rev. Phys. Chem. 47*, 369−395.
46. Hua, Q., Jia, W., Bullock, B. P., Habener, J. F., and Weiss, M. A. (1998) *Biochemistry 37*, 5858−5866.

47. Radhakrishnan, I., Perez-Alvarado, G. C., Dyson, H. J., and Wright, P. E. (1998) *FEBS Lett. 430*, 317−322.
48. Lee, H., Mok, K. H., Muhandiram, R., Park, K., Suk, J., Kim, D., Chang, J., Sung, Y. C., Choi, K. Y., and Han, K. (2000) *J. Biol. Chem. 275*, 29426−29432.
49. Ramelot, T. A., Gentile, L. N., and Nicholson, L. K. (2000) *Biochemistry 39*, 2714−2725.
50. Sayers, E. W., Gerstner, R. B., Draper, D. W., and Torchia, D. A. (2000) *Biochemistry 39*, 13602−13613.
51. Bairoch, A. (1999) http://ca.expasy.org/tools/pscale/A.A.SWISS−PROT.html.
52. Uversky, V. N., Gillespie, J. R., and Fink, A. L. (2000) *Proteins 41*, 415−427.
53. Romero, P., Obradovic, Z., Li, X., Garner, E. C., Brown, C. J., and Dunker, A. K. (2001) *Proteins 42*, 38−48.
54. Muñoz, V., Cronet, P., López-Hernández, E., and Serrano, L. (1996) *Folding Des. 1*, 167−178.
55. Viguera, A. R., Villegas, V., Avilés, F. X., and Serrano, L. (1996) *Folding Des. 2*, 23−33.
56. Taddei, N., Chiti, F., Fiaschi, T., Bucciantini, M., Capanni, C., Stefani, M., Serrano, L., Dobson, C. M., and Ramponi, G. (2000) *J. Mol. Biol. 300*, 633−647.
57. Schulman, B. A., Lindstrom, D. L., and Harlow, E. (1998) *Proc. Natl. Acad. Sci. U.S.A. 95*, 10453−10458.
58. López-Hernández, E., Cronet, P., Serrano, L., and Muñoz, V. (1997) *J. Mol. Biol. 266*, 310−620.
59. Chiti, F., Taddei, N., Webester, P., Hamada, D., Fiaschi, T., Ramponi, G., and Dobson, C. M. (1999) *Nat. Struct. Biol. 6*, 380−387.
60. Sheinerman, F. B., Norel, R., and Honig, B. (2000) *Curr. Opin. Struct. Biol. 10*, 153−159.
61. Kim, P. S., and Baldwin, R. L. (1982) *Annu. Rev. Biochem. 51*, 459−489.
62. Baldwin, R. L., and Rose, G. D. (1999) *Trends Biochem. Sci. 24*, 26−33.
63. Oas, T. G., and Kim, P. S. (1988) *Nature 336*, 42−48.
64. Staley, J. P., and Kim, P. S. (1990) *Nature 344*, 685−688.
65. Lumb, K. J., Carr, C. M., and Kim, P. S. (1994) *Biochemistry 33*, 7361−7367.
66. Fersht, A. R. (1997) *Curr. Opin. Struct. Biol. 7*, 3−9.
67. Buck, M. (1998) *Quart. Rev. Biophys.* 297−355.

BI015763T